C. R. Palevol 14 (2015) 219–232

Contents lists available at ScienceDirect

Comptes Rendus Palevol

www.sciencedirect.com

Human Palaeontology and Prehistory

Witnessing prehistoric Delphi by luminescence dating

Témoignage d'une Delphes préhistorique par la datation par luminescence

Ioannis Liritzis[a,*], Vassilios Aravantinos[b], George S. Polymeris[c,d], Nikolaos Zacharias[e], Ioannis Fappas[b], George Agiamarniotis[b], Ioanna K. Sfampa[f], Asimina Vafiadou[a], George Kitis[f]

[a] *University of the Aegean, Department of Mediterranean Studies, Laboratory of Archaeometry, Rhodes, Greece*
[b] *IXth Ephorate of Prehistoric and Classical Antiquities, Thebes, Greece*
[c] *Laboratory of Radiation Applications and Archaeological Dating, Department of Archaeometry and Physicochemical Measurements, 'Athena' - Research and Innovation Center in Information, Communication and Knowledge Technologies, Kimmeria University Campus, 67100 Xanthi, Greece*
[d] *Institute of Nuclear Sciences, Ankara University (AU-INS), Tandogan Campus, 06100 Ankara, Turkey*
[e] *Laboratory of Archaeometry, University of the Peloponnese, Department of History, Archaeology and Cultural Recourses Management, Old Camp, 24100 Kalamata, Greece*
[f] *Aristotle University of Thessaloniki, Nuclear Physics Laboratory, 54124 Thessaloniki, Greece*

ARTICLE INFO

Article history:
Received 19 June 2014
Accepted after revision 26 December 2014
Available online 14 April 2015

Handled by Marcel Otte

Keywords:
Prehistory
Delphi
Luminescence dating
Ceramics
Stones
SEM/EDS

ABSTRACT

A new research of prehistoric Delphi (Koumoula site, Parnassus Mountain) based on the absolute dating of an archaeological ceramic assemblage and stonewalls from recent rescue excavation is presented using luminescence techniques. For the chronological estimation of the ceramic assemblage, optically stimulated luminescence (OSL) and thermoluminescence (TL) protocols were employed, and the surface luminescence dating technique was applied on excavated calcitic rock samples. Dosimetry studies (field and laboratory) were practiced using a combination of a portable calibrated Geiger scintillator, alpha counting (pairs technique) set up and scanning electron microscopy (SEM/EDS), the latter also to probe information about the chemistry and firing conditions of the ceramics. The results of the study provided dates that ascribe the site to the Greek Neolithic and Early/Middle Bronze Age (~2000 to 5000 years B.C.), forming an absolute chronological framework for the studied area; moreover, these first prehistoric data provide archaeological links for the parallel use of the site with the nearby Corycian Cave habitation.

Mots clés :
Préhistoire
Delphes
Datation
Luminescence
Céramique
Pierres
MEB/SDE
Grèce

RÉSUMÉ

Une nouvelle recherche de la Delphes préhistorique (site de Koumoula, mont Parnasse) sur la base de la datation absolue d'un assemblage céramique archéologique et de murs en pierre provenant de fouilles récentes de sauvetage est présentée ici, en utilisant des techniques de luminescence. Pour l'estimation chronologique de l'assemblage céramique, des protocoles de luminescence stimulée optiquement (OSL) et de thermoluminescence (TL) ont été utilisés ; la technique de datation par luminescence de surface a été appliquée sur des échantillons de roches calcitiques extraites des fouilles. Des études de dosimétrie (terrain et laboratoire) ont été pratiquées en utilisant la combinaison d'un scintillateur Geiger

* Corresponding author.

http://dx.doi.org/10.1016/j.crpv.2014.12.007

calibré portable, d'un compteur alpha (technique des paires), de la microscopie électronique à balayage (SEM/EDS), cette dernière technique devant aussi fournir des informations quant à la chimie et aux conditions de cuisson des céramiques. Les résultats de l'étude ont fourni des dates remontant au Néolithique et au Bronze précoce à moyen (~2000 à 5000 ans B.C.) de Grèce, formant un cadre chronologique absolu pour la zone étudiée ; en outre, ces premières données préhistoriques fournissent des liens archéologiques en faveur d'un usage en parallèle du site ici étudié et de l'habitation voisine dite Antre corycien.

1. Introduction

Though the classical sanctuary of Delphi has been well studied, the earlier (prehistoric) times of settlement evolution of Delphi environs is poorly studied. The site of Koumoula up to Mount Parnassus occupies a prominent place on the so-called hill that emerges from the Livadhi valley in its southwestern part (Fig. 1a and b). Until a drainage work was undertaken sometime in later Prehistory (Knauss, 1987a,b, 122–127), the accumulation of waters, especially during wintertime, was changing periodically the plain into a spacious lake and the Koumoula hill in an island projecting over that. Since it is the only hill in the area, it attracted human habitation of farmers and shepherds who cultivated the fertile plain and used the surrounding slopes of Mount Parnassus for the grazing of their herds (Fig. 1).

Because of this human habitation, some building remains, lithics and lots of pottery sherds are now scattered on the entire surface of the Koumoula hill. Previous archaeological survey and trial excavations undertaken on the hill by the French School at Athens and the 10th Ephorate of Prehistoric and Classical Antiquities at Delphi yielded a number of pots and pottery sherds recognized as dating back to the Middle and Late Helladic periods (~1650–1100 years B.C.), as well as various stone, bone, and clay tools (Dasios, 1992: 87; Michaud, 1972, 912; Müller, 1992: 452, 490; Touchais, 1981: 95–172).

Earlier thermoluminescence (TL) dating was performed on three ceramics from the Corycian Cave, which lies in close proximity to the Koumoula site, indicating a dating to the 4th millennium B.C. (Liritzis, 1979; Touchais, 1981: 170). The Corycian cave has produced material and textural evidence of habitation from Upper Paleolithic to modern times, though over intermittent stages (Amandry, 1981).

In this work, luminescence dating is applied on the findings of Delphi prehistoric remains that include typical pottery sherds, as well as stone structures, using various methodological versions and techniques of luminescence (thermoluminescence and optically stimulated luminescence, both coined as surface luminescence techniques for rock surfaces). The aim is to produce a solid chronological frame of archaeologically undiagnosed ceramics and associated foundation walls, regarding their use and reuse, because the construction age of walls of a structure does not imply the same age of surrounding ceramic findings, and uttermost, to compare the end of this settlement with future planned dating of nearby seasonal lake sediments.

2. Luminescence dating

The absolute age of a historical or archaeological ceramic object is the most significant and useful piece of information, since this can be used to assist the characterisation of the site, as well as a crosscheck of the age of a building, structure, or settlement. Among the various dating techniques, luminescence stands as the most effective and well-established one towards the age assessment of heated/burnt materials (Aitken, 1985; Liritzis et al., 2013a). Moreover, in the case of a megalithic building or a stone artefact, the luminescence dating techniques have been well-documented (Liritzis, 2011; Liritzis et al., 2008; Theocaris et al., 1994, 1997; Vafiadou et al., 2007). Luminescence dating is based on the mechanism whereby minerals like quartz and feldspars act as natural dosimeters and preserve a record of irradiation dose, i.e. energy per unit mass received through time. This dose results mainly from the decay of natural radionuclides, i.e., ^{232}Th, ^{40}K, ^{87}Rb and natural U, along with cosmic rays, which provide a constant source of low-level ionizing radiation. The accumulated dose (equivalent dose in grays, ED) is stored by means of trapped charge in crystal defects, which is stable over long periods of time but can be released either by heating (thermoluminescence, TL) or exposure to sunlight (optically stimulated luminescence, OSL), while the luminescence signal intensity reflects the amount of trapped charge and is proportional to the time elapsed. Every time that the material is subjected to prolonged heating (as in the case of firing pottery) or intense light exposure (as in the case of sunlight), electrons are evicted and traps are emptied. In that case, the material is said to be totally zeroed. Afterwards, it could start accumulating energy in the form of trapped electrons in order to refill the empty traps once again.

Although TL is the most appropriate technique for dating kilns and pottery, OSL is also an effective method, especially in cases of limited sample in surface dating (Aitken, 1998; Liritzis et al., 2013a; Solongo et al., 2014; Thomas et al., 2008).

Towards the direction of age determination, two different physical quantities are required; the total accumulated dose during the past, termed as palaeodose or equivalent dose (ED), as well as the rate at which this energy-dose is accumulated, termed as dose rate (DR). The ratio of these two quantities, i.e. the palaeodose over the dose rate, represents the age of the sample:

$$\text{Age} = \frac{\text{Equivalent Dose (Gy)}}{\text{Dose Rate (Gy/ka)}} = \frac{\text{ED}}{\text{DR}}$$

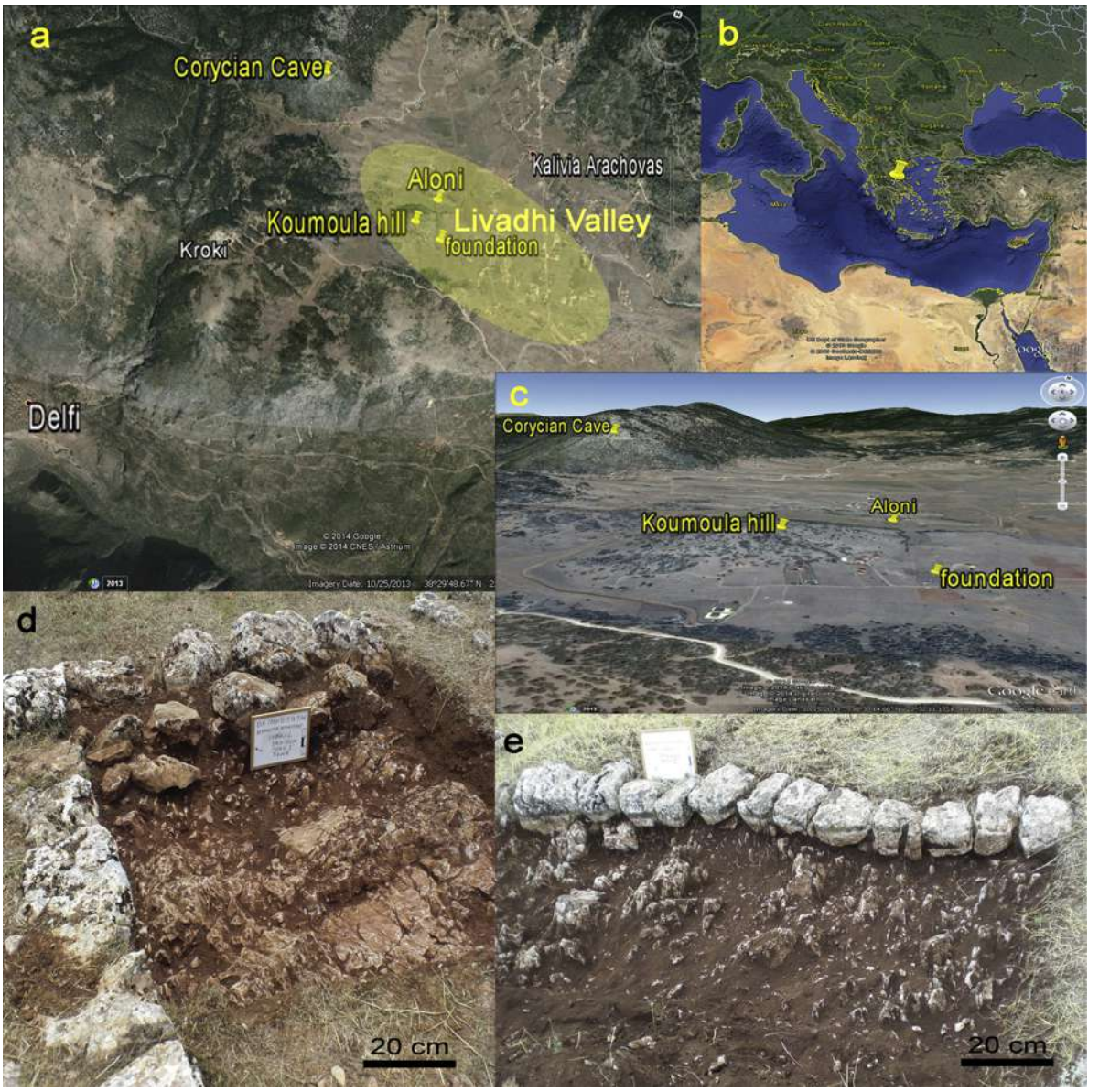

Fig. 1. (Color online.) Livadhi Valley and Koumoula hill (a, b, c) and the excavation site, at Granitsiotis' plot, section I (d), and at the "Aloni" area, section II (e).
Fig. 1. (Couleur en ligne.) Vallée de Livadhi et colline de Koumoula (a, b, c) et site de fouille, à l'endroit de la propriété Granitsiotis, section I (d) et dans la zone « Aloni », section II (e).

The most widely used method to estimate the absorbed dose rate is by measuring the sample's content of radioactive elements (^{40}K, ^{235}U series, ^{238}U series, and ^{232}Th series) and calculating the amount of radiation that these release per time unit. The calculation takes into account the possible presence of water as it attenuates ionizing radiation, and the amount of cosmic radiation that reaches the sample at a given depth below ground surface. The aim is to use the TL and OSL signals for determining the time that has elapsed since the ceramics were last fired, and since the surfaces of the rock samples were last exposed to sunlight, in the latter case yielding a construction age.

3. Analytic facilities

TL measurements were applied at the nuclear physics laboratory of the Physics Department, Aristotle University of Thessaloniki, Greece, using a Littlemore type 711 set up, with a P/M tube: EMI 9635QA bialkali (Sb K–Cs) and a thermo couple type: 90/10 Ni/Cr and 97/03 Ni/Al, filter transmitting in the 320–440-nm range. In all cases, a beta test dose was provided by a ^{90}Sr/^{90}Y beta source delivering 1.72 Gy/min. All TL measurements were performed in a nitrogen atmosphere with a constant heating rate of 2 °C/s in order to avoid significant temperature lag, up to a

maximum temperature of 500 °C. Mass reproducibility for all samples was kept within ± 5%.

OSL measurements were performed at the Laboratory of Radiation Applications and Archaeological Dating in Xanthi, using a Risø TL/OSL-DA-15 reader, equipped with a $^{90}Sr/^{90}Y$ beta source delivering 4.5 Gy/min. The reader was fitted with a 9635QA photomultiplier tube. The detection optics consisted of a 7.5-mm Hoya U-340 ($\lambda_p \sim 340$ nm, FWHM 80 nm) filter, transmitting in the 280–380-nm region, with maximum transmittance (57%) at 330 nm. An array of blue light emitting diodes (LEDs, 470 ± 30 nm) was used for stimulation, emitting 40 $mW \cdot cm^{-2} \cdot s^{-1}$ at the position of the sample. For IRSL, the stimulation wavelength is 875 (± 40) nm and the maximum power of ~ 135 $mW \cdot cm^2$ (Bøtter-Jensen et al., 1999a,b).

The annual dose of K for the ceramic samples was calculated after Scanning Electron Microscopy (SEM) measurements coupled with an Energy Dispersive Spectrometer (EDS), (Philips FEI-Quanta INSPECT with SUTW detector) at the Laboratory of Archaeometry of the Department of History, Archeology, and Cultural Resources Management, University of Peloponnese, Greece. The EDS system was set up for analysis with an accelerating voltage of 25 kV at a 35 take-off angle. An internal ZAF correction mode, in regard to the set up, was used to normalize the otherwise standardless analysis. Detection limits are within some decades of ppm; while the most reliable are those > 0.1%. For the surrounding soil, the K measurements were made with a Portable XRF, TN Spectrace 9000 with a mercuric iodide HgI_2 detector and three excitation sources of radioisotopes within the probe unit, Am-241 (26.4 keV K-line and 59.6 keV L-line), Cd-109 (22.1 keV K-line, 87.9 keV K- and L-line) and Fe-55 (5.9 keV K-line) (Liritzis and Zacharias, 2011).

A portable Radiagem 2000 (Canbera) Geiger was also used. Readings on counts/second were converted into mGy/yr after a successful calibration procedure based on radioactive pads and compared to a portable calibrated scintillometer NaI (Scintrex, model SPP-2).

Uranium-235 (and consequently U-238) and thorium-232 were measured by alpha counting employing the pairs technique assuming U-equilibrium at the Laboratory of Archaeometry, Department of Mediterranean Studies, University of the Aegean, Greece. The measurements were calculated using a 7286 Low-Level Alpha Counter, Littlemore Sci. Eng Co Oxford with a PM tube type EMI 6097B, calibrated in standards following devised conversion factors as well as relevant computations (Aitken, 1985; Liritzis and Vafiadou, 2012). The conversion to dose rates was based on the work by Liritzis et al. (2013b).

4. Samples, sample preparation and mineralogy

4.1. Samples

In 2010 a rescue excavation was undertaken at the site by the 9th Ephorate of Prehistoric and Classical Antiquities at Thebes. The excavation was conducted in two spots, on the summit of the hill, the so-called “Aloni” area made of ordered circular cobbles (Fig. 1e), and on its eastern slope, in the G. Granitsiotis’ plot (Fig. 1d), where the stone foundations of a large square building are still preserved and visible.

The samples that were chosen to be dated are seven pottery samples (D1–D8) (Fig. S1), and four stone samples (KoumF, KoumB, Aloni1, Aloni2) (Table 1). Pottery codes D1–D4 come from the “Granitsiotis” plot and D5–D8 from the “Aloni” top of the hill. Both spots yielded a restricted number of pottery sherds of various types and thicknesses, which mostly come from coarse ware, hand-made household prehistoric pots. Several of them are thin and much worn, implying that they underwent severe corrosion and alteration; finally, all assemblage fragments were in small dimensions and not decorated. Some of them, however, can be attributed, though with uncertainty, to the Middle Helladic period (2000–1700 B.C.), according to their shape, manufacture technology, firing, fabric, and surface treatment. Towards this dating also points the small stone tool—a flint comb—found together with the second pottery assemblage of D2 at Granitsiotis plot.

4.2. Sample preparation

Treatment and preparation for all samples were undertaken in subdued red-light conditions. For pottery, a 2-mm layer was removed from all sample surfaces to eliminate the light-subjected portions, followed by gently crushing in an agate pestle and mortar. The fine grains, between 4 and 11 μm, were separated from coarse grains by sinking them into acetone as the solvent according to the settling procedure described by Zimmerman (1971), without HCl pretreatment.

Stone samples were taken from closely joined carved cobbles of foundation wall and threshing stone floor with the aid of a hammer and chisel, exerting care to remove pieces of around 2 × 2 cm, preserving the original surface. Samples were swiftly wrapped in black plastic bags to avoid sun exposure. As an added precaution against light exposure, the sampling took place late in the evening while the adherent soil on the surface helped to prevent sunlight from reaching the surface (see also Liritzis, 2010; Vafiadou et al., 2007). The surface’s exposure time to sunlight depends on the time taken by the stonemasons to put a given block in the appropriate position overlaid by another. From the moment that any surface is no longer exposed to sunlight and put in firm contact with mortar, the luminescence signal starts to develop.

The original surface of the sample was cleaned, under red-light conditions, with diluted HCl acid to remove dust, and any organic residues and secondary salt by-products.

A gentle removal of a ~ 50 μm layer is made by a fast immersion to diluted HCl, repeated around five times (Liritzis et al., 1997). Fine powder sample is finally removed through a gentle rubbing of ×50 traverses of surface. A thin layer of surface powder was acquired by gently scraping the inter-block surface to a depth of less than 0.5 mm (making a series of readings with a micrometer) and transferred to an acetone bath where grains were collected, washed in dilute acetic acid (0.5%) for 1 min, and left to dry overnight in an oven at 50 °C. TL measurements were carried out following multiple aliquots made of the polymineral material on which the total bleach assumption was applied, which

Table 1
Luminescence data, sample number, method applied, temperature region used, recycling ratio (R.R.), recuperation, mean ED. Total dose rate and ages in B.C (bold, italic and asterisk see note [c] below).
Tableau 1
Données de luminescence ED, numéro d'échantillon, méthode appliquée, domaine de température, rapport de recyclage (R.R.), récupération, valeur moyenne des équivalents dose. Taux de dose totale et âges en AJC (pour le gras, italique et astérisque, voir la note ci-dessous [c]).

A/A	Sample[a]	Method	ED (Gy)	Temperature (°C)	R.R.	Recup. (%)	Mean ED	Total DR (mGy/y)	Age (B.C.)
Ceramics[b]									
1	D1	MAAD TL	18.9 ± 3.2 *31.7 ± 6.6	200–250 *260–360*	–	–	–	3.95 ± 0.28	2780 ± 1112 6018 ± 2177
2	D2	SAR OSL	18.1 ± 0.7	220–260 (n = 9)	1.07 (0.03)	5.5	–	3.95 ± 0.28	2586 ± 478
3	D4	SAR OSL	19.3 ± 1.3	220–260 (n = 9)	1.06 (0.04)	3.2	–	4.51 ± 0.32	2281 ± 583
4	D5	MAAD TL MAAD TL	28.5 ± 3.9 *69.4 ± 7.8	195–240 *285–355*	–	–	–	4.04 ± 0.28	5058 ± 1454 15186 ± 3120
5	D6	MAAD TL	20.9 ± 4.2 *41.0 ± 5.6	200–250 *270–310*	–	–	–	4.10 ± 0.29	3103 ± 1691 8011 ± 2003
6	D7	MAAD TL	24.4 ± 3.1	280–345	–	–	–	4.03 ± 0.28	4055 ± 1175
7	D8	MAAD TL	20.1 ± 3.5 *24.2 ± 4.2	240–330 *340–380*	–	–	–	4.10 ± 0.82	2898 ± 1171 3897 ± 1406
Prehistoric Building (Foundations) and Threshing floor[c]									
8	Aloni1-1	SAR OSL	8.352 ± 2.736	260(n = 3)	0.99 (0.17)	12.5	***7.68 (1.1)(1.47)***	1.76 ± 0.05	2430 ± 400[d]
9	Aloni1-1	SAR OSL	8.28 ± 2.736	260(n = 3)	0.91 (0.17)	8			
10	Aloni1-1	SAR OSL	6.408 ± 2.016	260(n = 3)	0.72 (0.18)	17			
11	Aloni1-2	SAR OSL	3.312 ± 0.864	260(n = 3)[e]	1.01 (0.11)	8	***4.37(1.03)(0.58)***		
12	Aloni1-2	SAR OSL	4.248 ± 1.296	260(n = 3)	1.09 (0.18)	13			
13	Aloni1-2	SAR OSL	5.544 ± 0.72	260(n = 3)	1.22 (0.20)	3.5			
14	Aloni2-1	SAR OSL	21.744 ± 2.808	260(n = 3)	0.96 (0.25)	6	*19.1(2.85)(1.65)*		
15	Aloni2-1	SAR OSL	16.056 ± 1.80	260(n = 3)	0.86 (0.12)	12			
16	Aloni2-1	SAR OSL	19.512 ± 3.528	260(n = 3)	0.91 (0.22)	4			
17	KoumF[f]	MAAD TL	7.97 ± 0.64	340–370	–	–			
18	KoumB	SAR OSL	5.328 ± 1.224	260(n = 3)	1.09 (0.18)	23	***5.69 (1.1) (0.63)***	1.55 ± 0.21	1670 ± 640
19	KoumB	SAR OSL	6.84 ± 0.936	260(n = 3)	1.12 (0.17)	14			
20	KoumB	SAR OSL	4.896 ± 1.08	260(n = 3)	1.30 (0.19)	22			

DR: dose rate; Recup.: recuperation; ED: equivalent dose.

[a] Pottery fragment labeled as D3, of dimensions 1 × 1.5 × 2 cm was excluded from the luminescence study due to its size limitations.

[b] In the case of MAAD, the temperature indicates the plateau region. In the case of SAR OSL, the temperature region indicates the preheat temperature applied. Variable n indicates the total number of aliquots measured. For the case of MAAD TL, secondary plateaus are indicated in italics with stars.

[c] Luminescence data for the ED estimation of four out of five samples. Three discs were measured for each sample. A typical SAR OSL protocol was applied, after using three regenerative doses of 10, 20, and 30 Gy. Preheating: 260 °C for 10 s. In the column "Mean ED", the first value stands as the mean value of the three independently measured EDs; the first parenthesis represents the error indicated from the standard deviation of the three values, while the second parenthesis indicates the error propagation analysis result based on the independent error of each measurement. For another sample, Aloni 2-2, the lack of a fast OSL component precludes the feasibility of OSL dating.

[d] For the age calculation, we used the mean ED from samples Aloni1-1 and KoumF.

[e] The number of aliquots was limited due to the very small powder quantity removed from rock surface.

[f] MAAD TL was used instead of SAR OSL because of very low quartz signal.

is only valid for cases where here the sample has been exposed to sunlight for a long duration (Liritzis et al., 1996, 2013a; Singhvi et al., 1982).

Fine grains of bi-mineral mix of calcium carbonate with quartz were acquired (polymineral fine grains), as XRD has shown, for further OSL measurements. In fact, 9-mm-diameter discs made of a 0.5-mm-thick aluminum substrate, each one containing ~2 mg of the sample (depending on the availability), were prepared. In some rock samples (Aloni threshing floor), the powder acquisition surface was divided into two sub-samples, i.e. in the unexposed surface, the acquisition of powder came from two different ranges, and from each one three disks were measured. This sub-area sampling is made to check possible destruction due to pressure/friction (earthquakes) or powder acquisition of visually unnoticed removed surface flake during sampling of parts of surface that may lead to an overestimated geological dose. Indeed the two carved blocks are not usually overlapping on their entire flat face, and any exerted pressure may cause friction in some parts, not in all, of the contact surfaces.

4.3. Mineralogy

On Fig. 2, backscattered images of the SEM analyses for the ceramic fragments D5, 6, 7 and 8 are shown. SEM

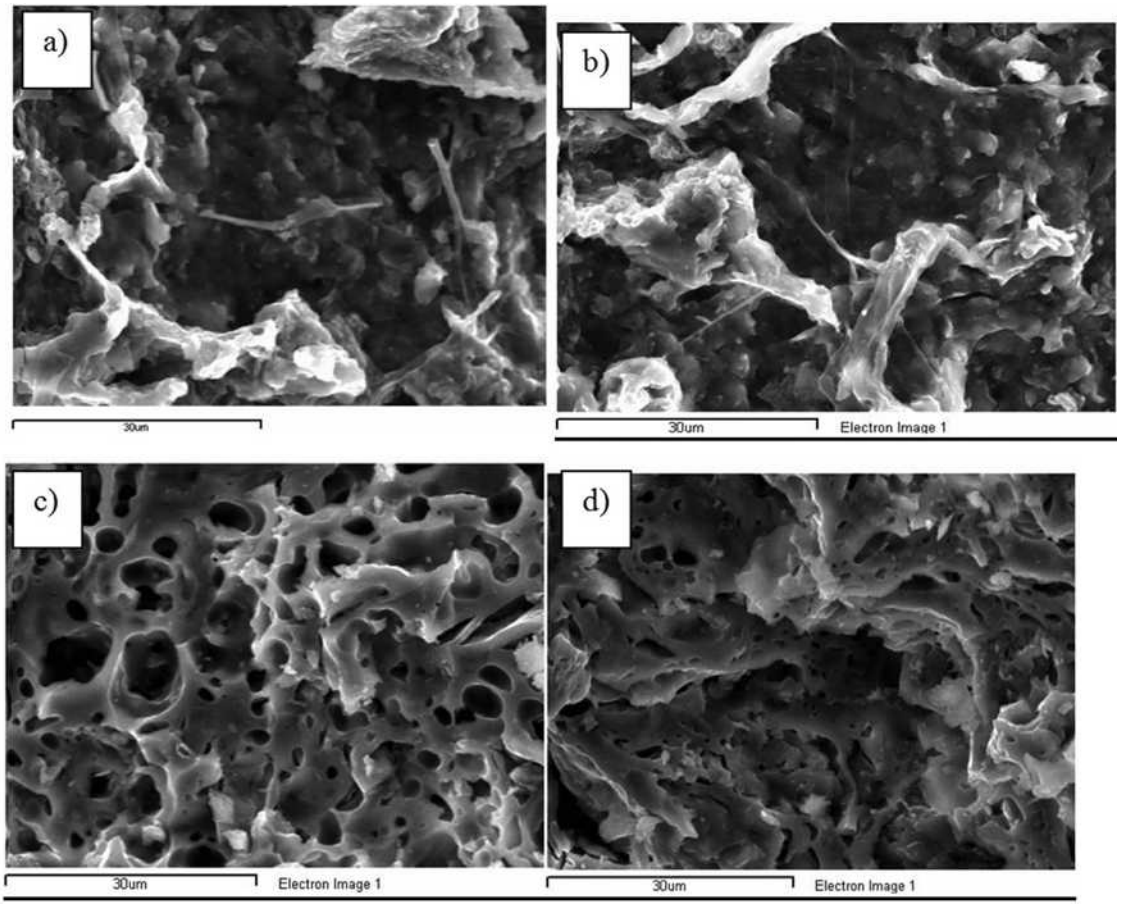

Fig. 2. Scanning electron microscopy images of the ceramic fragments using the backscattered mode (magnification 2000×): a: D5, low calcareous, biodegradation formations, with no signs of vitrification (temperatures below 800 °C); b: D6, medium calcareous, biodegradation formations, with no signs of vitrification (temperatures below 800 °C); c: D7, non-calcareous, signs of extensive vitrification, (temperatures between 850 and 1050 °C); d: D8, non-calcareous, signs of vitrification (temperatures between 850 and 1050 °C).
Fig. 2. Images au MEB de fragments de céramique en mode de rétrodiffusion (grossissement de 2000×): a: D5, formations biodégradées faiblement calcaires, sans aucun signe de vitrification (températures inférieures à 800 °C); b: D6, formations biodégradées moyennement calcaires, sans aucun signe de vitrification (températures inférieures à 800 °C); c: D7, non calcaires, avec signes de vitrification importants (températures comprises entre 850 et 1050 °C); d: D8, non calcaires, avec signes de vitrification (températures comprises entre 850 et 1050 °C).

images show signs of high-firing effects, especially for samples D7 and D8. The well-documented effect of cation exchange capacity for high- to over-fired calcareous pottery (Buxeda i Garrigos, 1999; Buxeda i Garrigos et al., 2002; Picon, 1976) has been reported in the literature as being responsible for chemical and mineralogical alterations resulting in a significant K leaching (Zacharias et al., 2005); this effect was also detected in cases of medium of even non-calcareous but high-fired pottery fragments (Zacharias et al., 2006a, Zacharias et al., 2006b), similar

Table 2
SEM/EDS data for the ceramic samples.
Tableau 2
Données SEM/EDS pour les échantillons de céramique.

A/A	Code name	Na_2O	MgO	Al_2O_3	SiO_2	SO_3	K_2O	CaO	TiO_2	Fe_2O_3	MnO
1	D1	nd	1.76	22.1	53.3	nd	2.02	2.92	1.98	15.9	nd
2	D2	0.66	1.51	20.83	59.51	nd	2.36	2.07	1.18	15.9	0.93
3	D5	nd	1.23	21.67	47.9	nd	3.74	2.79	0.92	18.35	nd
4	D6	nd	nd	26.23	49.52	0.35	3.16	4.12	1.04	18.35	nd
5	D7	nd	2.54	24.35	54.99	nd	2.53	1.34	1.05	13.25	nd
6	D8	0.46	0.89	20.33	49.88	nd	1.37	1.3	1.26	24.53	nd

SEM: scanning electron microscopy; EDS: energy dispersive spectrometer. Chemical compositions are given in wt% oxide; 'nd' denotes not detected.

to the present case, where mineralogical alterations and, mainly, potassium leaching effects have been documented. Although low in calcite (1.34 and 1.3 wt% in CaO for samples D7 and D8, respectively), the SEM patterns of samples D7, D8 show the presence of broad and extensive glassy formations (Fig. 2; Table 2). The vitrification is thus advanced, indicating temperatures of around 850–1050 °C (Maniatis and Tite, 1981). By considering the above discussion, the potassium value for sample D8 should be ignored as it may have undergone severe leaching during burial (see discussion in Supplementary Material). As a rule of thumb, an average potassium value of 2.86 ± 0.65%, taken from unaltered D5 and D6 samples, is considered as representative. The stones were calcites with traces of quartz confirmed by XRD (Liritzis et al., 2010).

5. Measurements and results

5.1. Equivalent dose estimation

Three different luminescence protocols were applied for the determination of the ED. These consist of the *multiple aliquot additive dose in TL* (*MAAD TL*, Aitken, 1985, 1998; Liritzis et al., 1997, 2001; Wagner, 1998), the single-aliquot regenerative dose in OSL (*SAR OSL*, Murray and Wintle, 2000) and the total bleach method in TL. The appropriate method was selected depending on each sample's nature (calcite, mix of calcite and quartz) and quantity (especially for the surface dating, where very few milligrams are recovered). Table 1 gives the analytical data resulted from the ED analyses.

5.1.1. Pottery

For five pottery samples (D1, D5–D8), the equivalent dose (ED) was determined after applying the *MAAD TL*. Each of these samples was divided into 16 separate discs and irradiated to regenerate an individual TL glow curve. In each study, samples were irradiated in groups of four discs at each dose. Four artificial doses of 4.12, 8.24, 12.36 and 24.72 Gy were attributed, depending on each sample's sensitivity.

In an attempt to verify ED, another luminescence protocol was applied, apart from *MAAD TL*, two out of the total seven pottery samples (D2, D4) were measured using the *single-aliquot regenerative dose (SAR)* protocol for OSL (Murray and Wintle, 2000). This method was also applied to the rock samples. Nine aliquots were measured from each one of the two pottery samples and three for each one among the five rock samples. Each disc was exposed to infrared radiation for 100 s at room temperature before laser stimulation, with the LED power held at 90%, i.e., 36 mW·cm^{-2}, in order to reduce the malign influence of any feldspar contamination grain to the signal (Wallinga, 2002). The post-IR OSL signals resulting from polymineral grains are believed to be dominated by the quartz signal (Banerjee et al., 2001; Roberts and Wintle, 2001; Zhang and Zhou, 2007). Feldspar presence in pottery was absent, thus the IR signal was zero. All signals are integrated over the first second of stimulation out of the 100 s of the entire curve. A background was subsequently subtracted based on the last 5 s (95–100 s) of stimulation. An example of OSL decay curves of the natural and the regeneration doses is presented on Fig. 3.

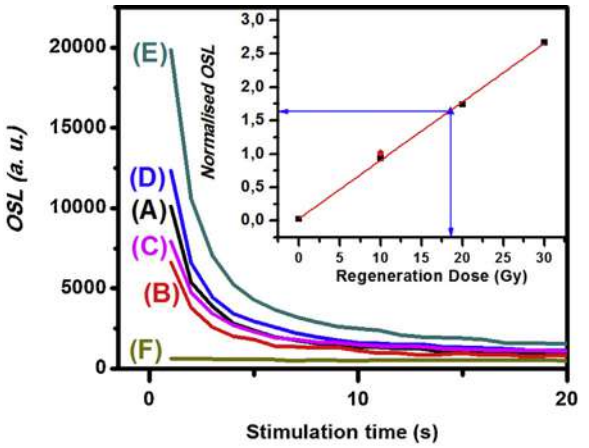

Fig. 3. (Color online.) Optically stimulated luminescence (OSL) decay curves for the natural signal (A), the three incremental regenerative doses, (C to E respectively), the repeat dose point (B) and the recuperation afterwards (F), for the first 20 s of stimulation. Inset: single-aliquot regenerative (SAR) growth curve, measured for an aliquot from the sample D4 after preheating at 220 °C. An equivalent dose value is provided by the interpolation of the natural normalised OSL signal (filled triangle) onto the growth curve (line) resulting from the fit to the results of the measurement sequence (filled squares). Filled dots represent the recycle point value; the SAR equivalent dose (ED) value yielded (line) is 18.9 Gy.

Fig. 3. (Couleur en ligne.) Courbes de décroissance de la luminescence stimulée optiquement (OSL) pour le signal naturel (A), les trois doses de régénération supplémentaires (C à E respectivement), le point de doses répétées (B) et la récupération après (F), pour les 20 premières secondes de stimulation. Encart: courbe de croissance SAR, mesurée pour une aliquote de l'échantillon D4 après préchauffage à 220 °C. La valeur de l'équivalent dose est fournie par interpolation du signal d'OSL naturel normalisé (triangle plein) sur la courbe de croissance (ligne) résultant de l'ajustement aux résultats de la séquence de mesures (carrés pleins). Le point plein représente la valeur du point de recyclage; la valeur SAR ED donnée (ligne) est de 18,9 Gy.

5.1.2. Stone

For all stone, but KoumF, samples, the ED was determined by *SAR OSL* measuring quartz in calcite. For KoumF sample, having mostly calcite and unmanageable low quartz signal, the *MAAD TL Dose-Temperature Plateau* approach was applied, used in earlier applications (Liritzis et al., 1997), and briefly described below. In fact, for the light-bleached stone materials, where the event to be dated is the last exposure to light, a modified additive dose procedure is used. The method involves the estimation of, and allowance for, the residual level of TL, assuming that its level was reduced to its minimum at the time of deposition. In that case, calculation of the equivalent dose involves subtracting this residual by extrapolating the dose response curve to the TL intensity of a natural aliquot that has received the total bleach.

The additive doses that were given were 42 Gy, 85 Gy, and 170 Gy (Fig. 4). Bleaching of TL curves was performed at different sunlight exposure hours. The Dose-Temperature Plateau Test was applied to find the starting level of NTL before overlaid by another stone. After each TL subtraction (Bg), a test dose of 6 Gy was made for normalization

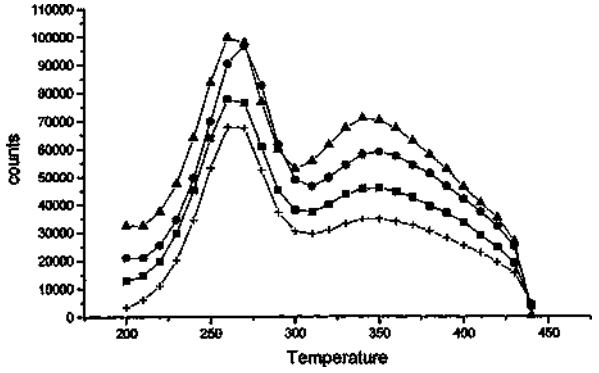

Fig. 4. Thermoluminescence curves for sample KoumF. Natural (crosses) and additive doses: 42 Gy (squares), 85 Gy (circles), 170 Gy (triangles).
Fig. 4. Courbes de TL de l'échantillon KoumF. Doses naturelles (croix) et doses additives 42 Gy (carrés), 85 Gy (cercles), 170 Gy (triangles).

purposes. Natural aliquots were bleached in sunlight for 6, 9, 10, 18 and 45 h. Similarly, the Equivalent Doses (ED) were obtained as with the previous method, by substituting the numerator with the subtraction of the remaining TL curves after different bleaching intervals of NTL. The bleached TL curves were subtracted from the corresponding natural, after which a built-up growth curve and a dose–temperature plateau were constructed (temperature between 200–350 °C, versus, ED, per each bleaching curve). The longest plateau represents the original (archaeological) TL curve, from which the environmental dose builds up. Experimental simulations elsewhere have evidenced this plateau (Liritzis, 2010; Liritzis and Bakopoulos, 1997; Liritzis et al., 1997, 2013a) (Fig. 7).

The ED was calculated from the equation:

$$\mathrm{ED} = \left(\Omega/((NTL + b) - NTL)\right) \times b,$$

where, Ω is the NTL (the natural TL) in the case of additive dose procedure for the ceramic samples, and NTL is the remaining TL after bleaching intervals; $(NTL + b)$ stands for the natural TL added beta doses curves and b the administered beta dose, in Gy.

In the *SAR OSL* technique, the signal intensity of an aliquot of extracted grains (called natural OSL) is recorded. After the measurement of the natural luminescence signal, each aliquot was given a series of increasing regeneration doses, in order to obtain a growth curve for each one. Three different regeneration doses were given for all cases, namely 10, 20, 30 Gy, in addition to a zero-dose check for the extent of recuperation (Aitken, 1998) and a repeat dose point in order to examine the adequacy of the test dose sensitivity correction procedure. The term 'regenerative dose' refers to the way the OSL growth function is regenerated under laboratory conditions.

Each OSL measurement removes electron charge from the excited levels and the laboratory irradiation regenerates quartz ability to show luminescence. Regeneration doses were chosen in order to bracket the equivalent dose yielded by the TL protocol. The preheat temperatures that were used were 200–260 °C for the pottery samples, based on the preliminary preheat plateau tests performed.

The SAR equivalent dose in all cases was then estimated by interpolation of the growth curve, as the dose required producing the natural signal. The growth curve was fitted for each aliquot by either a linear or a linear-plus-saturation-exponential growth function (see the inset on Fig. 3 for pottery and Fig. S2 for rock). For all preheats, heating rates were 2 °C/s.

Sensitivity changes induced by preheating, irradiation or optical stimulation were monitored and corrected with the aid of a test dose of 10 Gy, delivered after each regenerative or natural OSL measurement. Before each test dose measurement, a cut-heat at 160 °C was applied. The name "cut-heat" was adopted for the heating of the sample following each test dose, because the sample is immediately cooled after reaching the temperature. The success of the sensitivity test procedure was checked using another measurement cycle, using a regenerative dose equal to the first regeneration dose. The ratio of the corrected signals, the so-called "recycling ratio" (R.R.) (Murray and Wintle, 2000) indicates the efficiency of the sensitivity correction (Polymeris et al., 2009; Stokes et al., 2003). The zero-dose regenerative cycle is incorporated to measure any reverse charge transfer, known as recuperation, of charge previously photo-transferred to lower temperature traps due to preheating. Fading tests were not performed due to the fact that the Post-IR OSL signal from the pottery polymineral sample is dominated by quartz. In stone, no feldspars were present, but only traces of quartz (by XRD) though for safe line a double SAR protocol was applied. Nevertheless, in great agreement with the XRD results, the IRSL signals are flat, at the intensity level of the signal background. Recovery tests, as well as recycling ratios and recuperation provided satisfactory results.

5.1.3. *Equivalent doses: ceramic samples*

For the case of pottery samples, natural glow curves could be divided into two individual groups; the first one consisting of samples D1 (Granitsiotis house) and D5 (Aloni top), since they both yield a similar glow curve as is presented in the left plot on Fig. 5. The second category includes samples D6, D7 and D8 (all from Aloni top), since the corresponding glow curves consist mainly of two overlapping peaks, the first at around 250 °C and the second at around 375 °C. Another case comprises a separate set due to the application of the OSL method and includes samples D2 and D4 (both from Granitsiotis house). Fig. 5 shows characteristic glow curves of the additive dose procedure for two groups of samples. The left plot on Fig. 5 corresponds to sample D1, while D5 presents a similar glow curve too. On the other hand, right plot of the same Fig. 5 presents a characteristic example of the second group of samples and is coming from sample D7.

Equivalent doses were calculated within 1σ errors and are plotted against glow curve temperature for two samples on Fig. 6.

The TL signal provides adequately wide plateaus, over 50 °C in length. Equivalent dose values are plotted against glow curve temperature. TL peaks were not similar in each ceramic sherd but appeared at ~230 °C, ~280 °C and ~380 °C. The equivalent dose plateau test indicates wide plateaus, ranging in some cases from 200 to 250 °C and

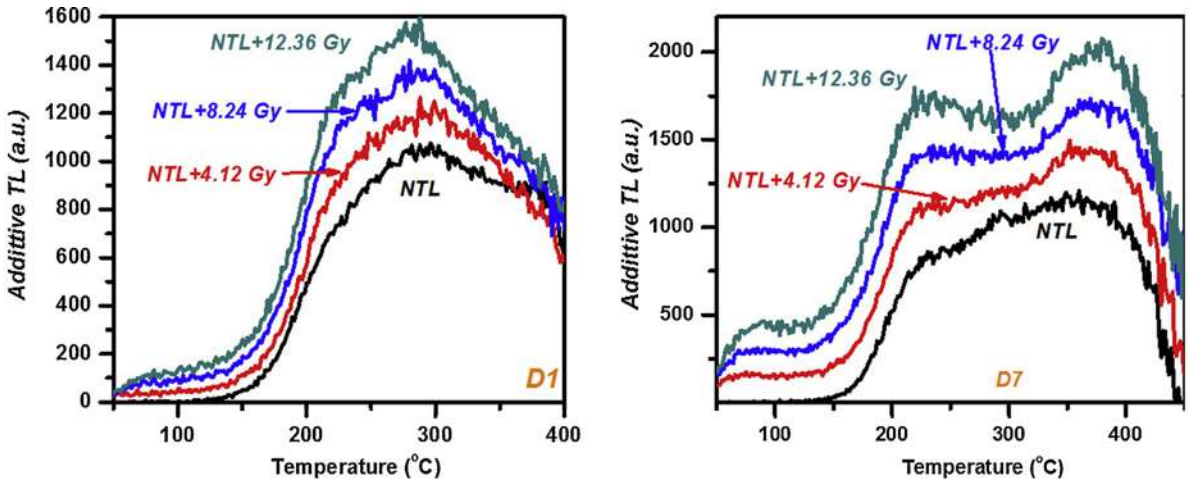

Fig. 5. (Color online.) (Left) Natural and natural-plus-beta dose glow curves for sample D1. The additive doses delivered were 4.12, 8.24, and 12.36 Gy. Reheats have been subtracted. The plotted natural thermoluminescence (NTL) is the average of four individually measured NTLs. NTL-plus-beta glow curves are the averages of three individually measured glow curves. (Right) Natural and natural-plus-beta dose glow curves for the sample D7. The additive doses delivered were 4.12, 8.24 and 12.36 Gy. Reheats have been subtracted. NTL plotted is the average of four individually measured NTLs. NTL-plus-beta glow curves are the average of three individually measured glow curves.

Fig. 5. (Couleur en ligne.) (Gauche) Courbes de préchauffage de doses naturelles et dose naturelle-plus-bêta pour l'échantillon D1. Les doses d'additifs livrés étaient de 4,12, 8,24 et 12,36 Gy. Les réchauffages ont été soustraits. La NTL tracée est la moyenne de quatre NTL mesurées individuellement. Les courbes de préchauffage NTL plus bêta sont la moyenne de trois courbes de préchauffage mesurées individuellement. (Droite) Courbes de préchauffage de doses naturelles et naturelles plus bêta pour l'échantillon D7. Les doses additives étaient de 4,12, 8,24 et 12,36 Gy. Les réchauffages ont été soustraits. La NTL tracée est la moyenne de quatre NTL mesurées individuellement. Les courbes de préchauffage NTL plus bêta sont la moyenne de trois courbes de préchauffage mesurées individuellement.

in some others on 300–350 °C. The equivalent doses were obtained as the mean values of the best plateaus for each sample. Errors derived mainly from the uncertainties in curve fitting, are $\pm 1\sigma$ and were calculated by standard error propagation analysis (Knoll, 1999). Regarding the low temperature TL peak range the 230 °C TL trap is typically found in many quartz samples. The TL signal from this trap has been used successfully in several comprehensive studies (see for example Bailiff and Holland, 2000; and references therein). The precision of the 230 °C additive TL method is excellent for doses above 0.1 Gy. It appears to be more accurate and more precise than the corresponding additive TL methods using the 330 °C and 370 °C peaks (Pagonis et al., 2011). Probably this has to do with the

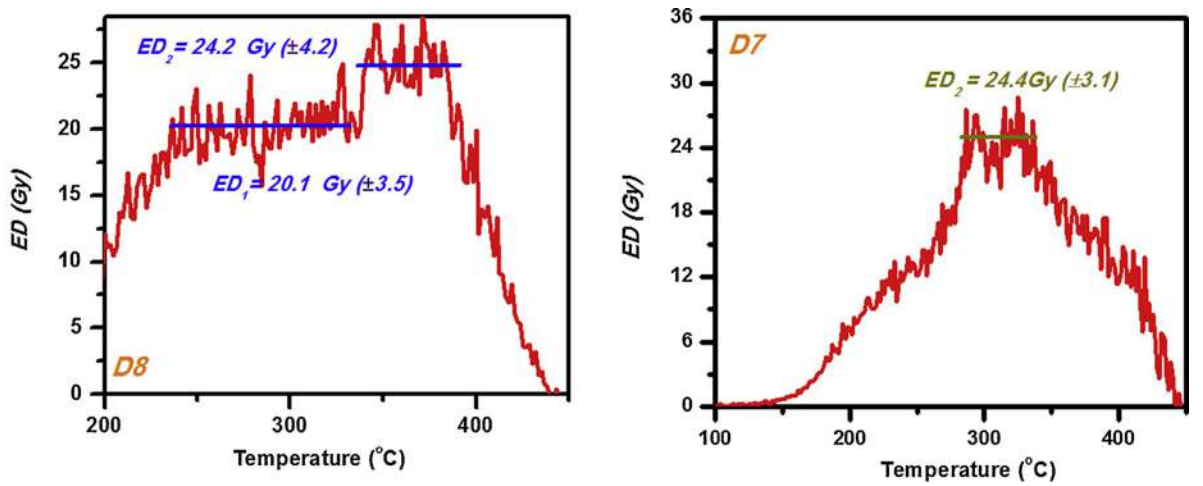

Fig. 6. (Color online.) (Left) Equivalent dose plateau plotted against the glow curve temperature for sample D8. The best plateau was found somewhere in the range between 240 and 330 °C. However, a second equivalent dose plateau was observed in the temperature region between 340 and 380 °C. (Right) Equivalent dose plateau plotted against glow curve temperature for sample D7. The best plateau was found in the range between 280 and 330 °C.

Fig. 6. (Couleur en ligne.) (Gauche) Plateau de l'équivalent dose en fonction de la température de la courbe de préchauffage pour l'échantillon D8. Le meilleur plateau a été trouvé dans une zone comprise entre 240 et 330 °C. Cependant, un second plateau d'équivalent dose a été mis en évidence dans une zone de température comprise entre 340 et 380 °C. (Droite) Plateau de l'équivalent dose en fonction de la température de la courbe de préchauffage pour l'échantillon D7. Le meilleur plateau se place dans une gamme de température comprise entre 280 et 330 °C.

firing conditions in antiquity (max temperature, re-firing, etc.). A summary of the TL dating data is given in Table 1, which presents the division of ED values into two groups regarding similar clusters of plateau. Group 1 consists of samples D1, D2, D4, D6, and D8 (1st plateau), with respective lower dose plateau values, which present an average of $ED_1 = 19.5 \pm 1.3$ Gy. Group 2 consists of samples D5, D7, and D8 (2nd plateau) with respective higher dose plateau values, which present an average of $ED_2 = 25.8 \pm 2$ Gy. A very interesting feature was yielded while estimating the ED values for the case of the ceramic samples using TL. For the majority of the samples, a second plateau is observed in the corresponding plots of equivalent dose versus temperature. This secondary plateau is observed at higher temperatures than that of the primary and main plateau, corresponding at the same time to a larger equivalent dose. This plateau is prominent in the case of sample D8, corresponding to an ED value of 24.2 (±4.2) Gy. These two plateaus are presented in the left plot of Fig. 6. Besides sample D5, which yielded a secondary ED value of 61.5 Gy, three more ceramic objects yielded equivalent doses in the range between 30 and 40 Gy. These high ED considered out of the expected archaeological range and may represent the geological dose or unknown crystal sensitivity inadequacy. The results dealing with these secondary plateaus are presented in tabulated form in Table 1.

An illustrative diagram of a SAR growth curve for an aliquot from the sample D4 is plotted in the inset on Fig. 3.

A summary of the OSL dating data is also given in Table 1. It is assumed that a laboratory-regenerated OSL signal grows in the same way as in natural conditions when quartz grains were cut-off from light after having been buried in soil or sediment. These laboratory irradiations and OSL measurements form the basis for establishing an individual growth function for the aliquot, which is then used to express the natural OSL in units of Gy of radiation dose absorbed by grains (see Figs. 3 and 10 and S2).

In the case of the ceramic samples, it is obvious that ED values yield a mean value of 21.5 Gy. Both TL and OSL present similar results, thus enhancing the validity of the results. The error is about 3 Gy for the TL case, which corresponds to less than 14%, while for the OSL case, the error is of almost 1 Gy, which means less than 5%.

5.1.4. *Equivalent doses: prehistoric building and threshing floor*

The glow curves from sample KoumF are shown in the following diagrams. Specifically, Fig. 4 presents the glow curves from the MAAD protocol, natural glow curves (average from three disks, crosses) and the additive doses of 42 Gy (squares), 85 Gy (circles), and 170 Gy (triangles). Fig. S3 shows the bleached curves and Fig. 7a the best plateau and the ED estimation.

As these data are not conclusive, since the estimates EDs were at 13–30 Gy for a temperature of 310–400 °C, the dating was repeated with regeneration of multiple aliquots, i.e. through adding beta doses to NTL and subtracting the remaining ones from bleaching cycles. Regenerative doses were 6, 11, 23, 34 and 56 Gy (test norm dose 6 Gy) (Fig. 8).

This is apparent from an additional bleaching cycle made under a SOL simulator for 30 h of equivalent sunlight exposure. The TL curve is shown on Fig. 9 together with the 18-h TL curve and the mean value of NTL. The 18-h curve almost coincides with natural. The ED is equal to 3.38 ± 0.50 Gy (Fig. 7b).

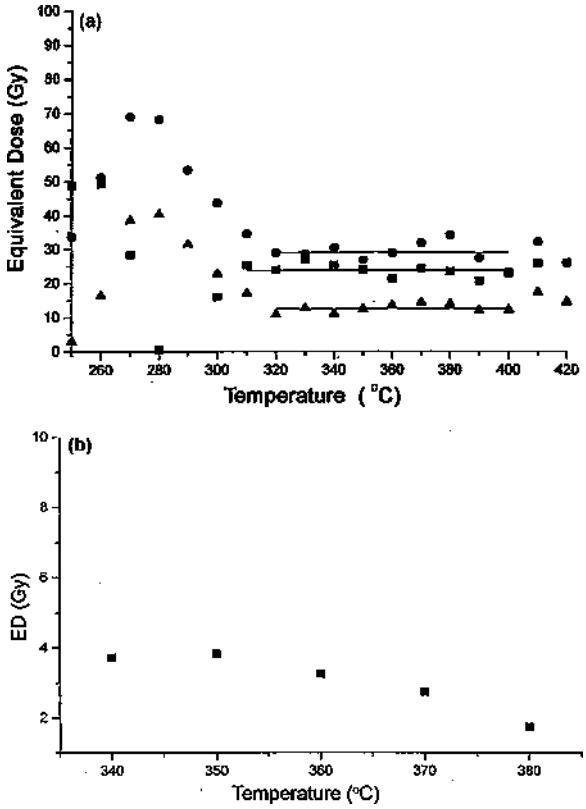

Fig. 7. a: equivalent dose (ED) results obtained using the method of total bleaching for sample KoumF; the resulted Dose Plateau test for 6, 9 and 18 h. Best plateaus are shown with flat lines with values at 13–30 Gy for $T \sim 310$–400 °C; b: ED of dose-temperature plateau following multiple aliquot additive dose (MAAD) for sample KoumF, for an exposure time ~30 h of equivalent sunlight (the time for which it was exposed in antiquity prior to its placement in situ and overlaid by another stone).
Fig. 7. a: équivalent dose ED issu du procédé de blanchiment total pour l'échantillon KoumF; résultat du test plateau–dose acquis pour 6, 9 et 18 h. Le meilleur plateau est représenté par des lignes plates, avec des valeurs à 13–30 Gy pour $T \sim 310$–400 °C; b: équivalent dose (ED) du plateau dose–température selon MAAD pour l'échantillon KoumF pour un temps d'exposition d'environ 30 h d'équivalent soleil (temps d'exposition dans l'Antiquité, avant le placement in situ et le recouvrement par une autre pierre).

Figure S4 in Supplementary Material shows the bleaching time versus the equivalent dose and the plateau length versus the bleaching time for stone powder KoumF. The maximum length of temperature vs. bleaching time plateau appears after ~25 h, which corresponds to ~8 Gy.

Aloni1 and 2 were divided into two sub-samples, and from each one three disks were measured. From the five samples from the threshing floor, four of them gave EDs. Sample KoumB was also divided into three disk samples, which all gave EDs. In the case of Aloni 2-2 samples, the natural OSL curves were problematic, due to the lack of a fast OSL component. Natural OSL (NOSL) signal was investigated and found to consist of one component, whose shape is rather peculiar and extremely flat, with intensity as large

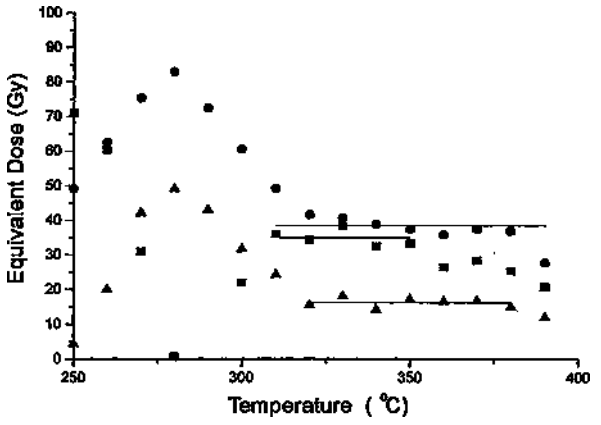

Fig. 8. Curves of regeneration of the equivalent dose doses (ED) for sample KoumF, for sun exposure durations of 6 h (■), 9 h (●), 18 h (▲). Flat lines are best plateaus of 16–38 Gy.
Fig. 8. Courbes « équivalents doses » (ED) de régénération pour l'échantillon KoumF, pour des temps d'exposition au soleil de 6 h (■), 9 h (●) et 18 h (▲). Les lignes droites représentent les meilleurs plateaux de 16–38 Gy.

as 2–3 times the OSL background signal. This is exactly similar to a CW-OSL tail after artificial irradiation. This NOSL signals for samples Aloni 2-1 and Aloni 2-2 are presented in the inset on Fig. 10, together with a background OSL signal for comparison.

In every case, we have to note the poor signal-to-noise ratio of the OSL curves. The EDs that were estimated from the rest of the samples are summarized in Table 1. Fig. 10 shows the OSL decay curves for the natural signal (NOSL), the three incremental regenerative doses (first, second and third R.D., respectively) and the recuperation afterwards (Rec), for the first 20 s of stimulation for sample Aloni2-1; an illustrative diagram of a SAR growth curve corresponding to the OSL curves is plotted as well on Fig. S2. It should be emphasized that both recycling ratios as well as recuperation values are quite high. This experimental feature could be attributed either to the fact that the samples were not heated or to the less quartz quantity of each bi-mineral

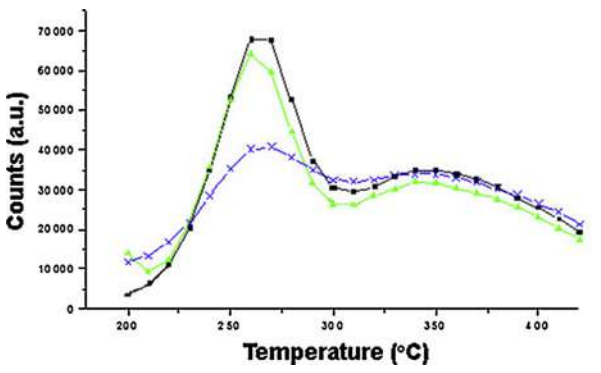

Fig. 9. (Color online.) Bleaching thermoluminescence curves of sample KoumF. Black color is mean natural, blue color corresponds to 30 h (SOL), and green color to 18 h under natural light.
Fig. 9. (Couleur en ligne.) Blanchiment de courbes de TL de l'échantillon KoumF. Couleur noire est naturel moyen, la couleur bleue correspond à 30 h (SOL) et la couleur verte à 18 h de lumière naturelle.

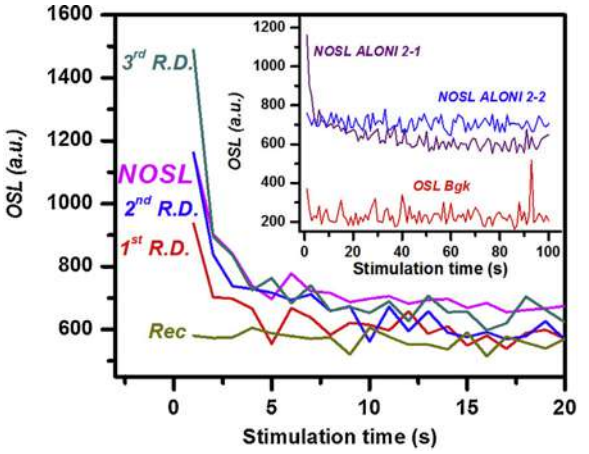

Fig. 10. (Color online.) Typical optically stimulated luminescence (OSL) decay curves for the natural signal (NOSL), the three incremental regenerative doses (1st, 2nd and 3rd R.D. curves, respectively) and the recuperation afterwards (Rec), for the first 20 s of stimulation. Inset: NOSL decay curve for the entire stimulation duration for the samples Aloni 2-1 and Aloni 2-2. Note the poor signal-to-noise ratio of the OSL curves.
Fig. 10. (Couleur en ligne.) Courbes de décroissance de la luminescence stimulée optiquement (OSL) typiques pour le signal naturel (NOSL), les trois doses de régénération supplémentaires (1re, 2e et 3e courbes R.D., respectivement) et la récupération après (Rec), pour les 20 premières secondes de stimulation. Encart: Courbe NOSL de décroissance pour la durée entière de stimulation pour les échantillons Aloni 2-1 et Aloni 2-2. À noter le mauvais signal quant au rapport signal/bruit des courbes d'OSL.

sample. Summarizing, the estimated ED for the foundations of the prehistoric building from sample KoumB is 5.69 ± 1.1 Gy. For the threshing floor, from the three EDs that were obtained from the samples Aloni1-1, Aloni1-2, and Aloni2-1, the value 7.68 ± 1.1 Gy is similar to that of 7.97 ± 0.64 Gy, estimated with the TL and the MAAD protocols. Thus, the ED for the floor is taken as the average of those two values, i.e. 7.8 ± 0.8 Gy. Other higher doses (Aloni2-1) represent a geological signal rising from deeper layers during sampling or caused by friction during the past and have been excluded.

5.2. Dose rates

The results for the annual dose rate measurements for all the samples and the surrounding soil and the total Dose Rate estimation for the samples are summarised in Table 3. The value of the alphas/betas efficiency was adopted to be 0.1 (Polymeris et al., 2011), the cosmic ray dose rate of 0.20 mGy/yr (estimated as per Prescott and Hutton, 1988), the internal quartz dose rate 0.1 mGy/yr is assumed; finally, for the overlaid stones, half the beta dose rate is considered, because a surface layer of about 50 μm is removed by diluted acid, and due to the thin layer of paste between them, only the beta particles from the lower (sampled) block are accounted for.

Gamma ray dose rates plus cosmic ones ranged from 0.8 to 1.1 mGy/yr. A similar result was deduced from calculations of individual radiation components of cosmic + rock + ground soil of the almost 2π counting geometry.

Table 3
Chemical analysis and total dose rate for all the samples.
Tableau 3
Analyse chimique et taux de dose totale pour tous les échantillons.

Sample	U (ppm)	Th (ppm)	K_2O	Water content (%)	Total DR (Gy/ky)
D1	1.71 ± 0.2	7.16 ± 0.75	2.02	20	4.10 ± 0.82
D2	2.1 ± 0.22	5.46 ± 0.76	2.36		
D4	3 ± 0.29	9.46 ± 1.03	n.m.		
D5	1.67 ± 0.24	8.48 ± 0.9	3.74		
D6	2.105 ± 0.25	7.48 ± 0.65	3.16		
D7	2.04 ± 0.23	6.84 ± 0.84	2.53		
D8	2.116 ± 0.25	7.55 ± 0.72	1.37		
Surrounding soil	2.57 ± 0.27	5.5 ± 0.94	1.68		
KoumB	0.12 ± 0.02	0.14 ± 0.06	0.06	20	1.55 ± 0.21
Koumoula soil	3.02 ± 0.24	6.25 ± 0.77	1.68		
ALONI	0.12 ± 0.03	0.14 ± 0.08	0.06	20	1.76 ± 0.05
KoumF	0.12 ± 0.01	0.13 ± 0.03	0.06		
Aloni soil	2.57 ± 0.25	5.5 ± 0.94	1.68		

The Rb value was estimated by the ratio Rb/K = 1/200; the average K of samples D5 and 6, of 2.86%, was used for the calculations of the final dose rate in the case of ceramics (see text, section 6); DR: dose rate; n.m.: not measured.

6. Discussion

The online supplementary figures give representative images of ceramic fabric sherds and the flint comb (Fig. S1), typical OSL decay curves recuperation and regeneration curves, and SAR growth curves and ED evaluation of the growth curve. A low signal-to-noise ratio must be particularly noticed for rock samples (Fig. S2), as well as bleached TL curves for various light-exposed periods (6 to 45 h) (Fig. S3), and the bleaching time vs. equivalent dose with the determination of maximum length of temperature—dose plateau, derived from various sun bleaching times (3 to 45 hours). A ~25-h bleaching time was chosen, which corresponds to an equivalent dose of ~8 Gy.

Estimations of ED values obtained using the SAR protocol are very insensitive to changes in all the potential measurement parameters; in particular there is no systematic dependence on preheat temperature over a wide range or on stimulation temperature. A preheat plateau test was performed. No differences were obtained in EDs in concordance to Murray and Wintle's (2000) comments. Regarding TL peaks, the ceramics present diversity albeit they come from the same sites—a glow curve with 230 °C peak and two overlapping peaks at ~250 °C and ~375 °C, while in two cases, application of the OSL method was made. Amongst the acceptable EDs two sets are separated as they fall within 2σ (19.5 ± 1.3 Gy and 25.8 ± 2 Gy). In dose rates, the radioactivity measurements of each ceramic sample were used with a common environmental gamma ray dose rate, and for the stones average radioactivity data were employed.

The derived ages (Table 1) of the seven ceramic samples range between the beginning of 5th to the late 3rd millennium B.C., but in three ceramic sherds, i.e. D1, D5 and D6, a secondary plateau gave a higher age between the 15th and the 7th millennia B.C. These higher EDs obtained for higher temperature peaks are considered out of the expected archaeological range and may represent geological dose or unknown crystal sensitivity inadequacy. The accepted estimated age derived from reliable measurements, as the applied reliability criteria were satisfied in both SAR and MAAD measurements, and the apparent few differences are due to other reasons linked to the materials, not related to the methods. Thus, overall we attribute them to the Late Neolithic to Early Bronze period (ca. 4800–ca. 2000 B.C.), and using the EDs from the two groups of the ceramics, the chronological result that is obtained falls within the end of 5th and mid-beginning of the 3rd millennium B.C. This comes in contrast to the archaeological estimation, which, with uncertainty though, due to the small and unpainted pottery fragments, leads us to attribute them to the Middle to the Late Bronze Age (ca.2000–1050 B.C.).

Table 4
The estimated dates.
Tableau 4
Dates estimées.

Sample	Date (B.C.)	Archaeological date
Ceramic	4550 ± 780 2730 ± 490	Middle/Late Neolithic period Early Bronze Age
Threshing floor	2430 ± 400	Early Bronze Age
Prehistoric building foundations	1670 ± 640	Middle/Late Bronze

Regarding the stone foundations, the ages obtained represent the last use/rebuilt of the stone masonry with ages at the Mid/Late Bronze Age (Table 4). Due to the inhomogeneous nature of limestones, variations were obtained in TL, OSL and criteria test from the two rock masonries and within the same cobble. The low recycling ratio and recuperation rates for Aloni1-1 (0.72, 17%) and Aloni 2-1 (0.86, 12%), as well as the high ones for KoumB (1.30, 22%), are noticeable (Table 1). High ED for Aloni2-1 implies the participation of geological TL from deeper layers or sampling of parts of the surface from which the original layer was absent (due to friction during placement of the two blocks or due to sometime during past, or when the piece was cut and removed from the block).

These dates are in accordance with those in which the nearby Corycian Cave was in use, indicating that the habitation of Koumoula hill was expanding over a very large

period of time, while the parallel use of both sites should not be excluded. The two dose plateaus obtained for D1, D5, D6, and D8 (Table 1) could imply accidental re-firing at temperatures lower than 300 °C at a later (Bronze Age) period. This is supported by the ceramic group at Granitsiotis house; amongst the findings were five pieces of low temperature-baked clay not fired on purpose (assemblage of D4), bearing traces of litter; maybe they derived from the wall or roof coating. Traces of fire are also speckled with the soil clays and become abundant in the western half of the excavated section with their eastern boundary close to the adjacent stone foundation. Some sherds were encountered in an adjacent excavated section, but traces of burning continue to deeper layers towards the stone foundation. An early stage of Middle Bronze (ca. 2100–1900 B.C.) date is supported by the stone scraper (flint) found there, as this is a typical tool of the period. Thus, possible re-uses are strongly supported by the ages provided by the second ED plateaus of TL at higher temperatures, hereafter termed as older ages. Although at the "Aloni" top of the hill no traces of fire were detected during the rescue excavation, but rather a plethora of cobbles and soil was found, the accidental or purposeful burning of the site cannot be precluded. Especially, in the case of sample D8 from "Aloni", the two ED plateaux correspond to ages of $\sim 2900 \pm 550$ B.C. and $\sim 3900 \pm 1400$ B.C. This older age stands in agreement with the age of 4000 ± 1170 B.C. of D7 of the same location. The younger ages for the other samples that exhibit two plateaus are not methodological error of luminescence; they represent rather poorly fired ceramics and support the argument of re-habitation, re-occupational phases of the site that ended after its destruction. Having said about the qualitative argument that the ceramics were poorly (re-?)fired, on the other hand it should be stressed that the numerical information derives from criteria tests, different protocols, complementary instrumentation and techniques applied to the same end, which strengthens the reliability of the obtained age results.

The impact of the results on the archaeological interpretation of the evolutionary process of the region has to do with the preceding habitation of the later Delphi sanctuary with the famous oracle, and the local settlement continuation following the Neolithic Corycian Cave—a cave mentioned by the 2nd-century-AD historian and traveller Pausanias (*Paus. 10.32.2*, in Jones and Ormerod, 1918).

A related key-question that arises through this study is whether Livadhi valley forms an infill of sediments related to an ancient flood, whose later myths were attributed to Deucalion.

In any case, the continuation of the excavations scheduled for the coming years, is of great importance in order to shed more light on the site's occupational and geoarchaeological layers and to provide new material for further analytical studies.

7. Conclusion

Prehistoric Delphi remains evidenced from Koumoula settlement on the Parnassus Mountain on the Livadhi valley have been assessed by surface and traditional luminescence dating. The luminescence protocols of MAAD and SAR were followed and applied in a systematic way for the estimation of the luminescence ages. The chronological range that is obtained for the architectural (foundation of walls and stone floor) and archaeological (not typologically diagnosed ceramics) remains falls within the late 5th and 3rd millennia BCE. The interpretation of the age data suggests re-habitation and re-occupational phases of the site.

Acknowledgments

The authors acknowledge the permission for the excavation and the scientific study of the material provided by the 9th Ephorate of Prehistoric and Classical Antiquities, Ministry of Culture, Greece, and Robert Temple for funding the project.

Appendix A. Supplementary data

Supplementary data associated with this article can be found, in the online version, at http://dx.doi.org/10.1016/j.crpv.2014.12.007.

References

Aitken, M.J., 1985. Thermoluminescence Dating. Academic Press, London.
Aitken, M.J., 1998. An introduction to Optical Dating. Oxford University Press, Oxford.
Amandry, P., 1981. L'Antre corycien dans les texts antiques et modernes. Bull. Corresp. Hell., Supp. 7, 29–54.
Bailiff, J.K., Holland, N., 2000. Dating bricks of the last two millennia from Newcastle upon Tyne: a preliminary study. Radiat. Meas. 32, 615–619.
Banerjee, D., Murray, A.S., Bøtter-Jensen, L., Lang, A., 2001. Equivalent dose estimation using a single-aliquot of polymineral fine grains. Radiat. Meas. 33, 73–94.
Bøtter-Jensen, L., Duller, G.A.T., Murray, A.S., Banerjee, D., 1999a. Blue light emitting diodes for optical stimulation of quartz in retrospective dosimetry and dating. Radiat. Prot. Dosim. 84, 335–340.
Bøtter-Jensen, L., Mejdahl, V., Murray, A.S., 1999b. New light on OSL. Quat. Sci. Rev. 18 (2), 303–309.
Buxeda i Garrigos, J., 1999. Alteration and contamination of archaeological ceramics: the perturbation problem. J. Archaeol. Sci. 26, 295–313.
Buxeda i Garrigos, J., Mommsen, H., Tsolakidou, A., 2002. Alterations of Na, K and Rb concentrations in Mycenaean pottery and a proposed explanation using X-ray diffraction. Archaeometry 44, 187–198.
Dasios, F., 1992. Contribution to the topography of ancient Phocis. Fokika Chronika 4, 18–95 (in Greek).
Jones, W.H.S., Ormerod, H.A., 1918. Pausanias Description of Greece with an English Translation in 4 Volumes. Harvard University Press/William Heinemann Ltd, Cambridge, MA/London.
Knauss, J., 1987a. Deukalion, die grosse Flut am Parnass und der Vulkanausbruch von Thera. AW 18/3, 23–40.
Knauss, J., 1987b. Die Melioration des Kopaisbeckens durch die Minyer im 2. Jt. v. Chr. Kopais 2: Wasserbau und Siedlungsbedingungen im Altertum; generelle Forschungsergebnisse 1985–87. München Lehrst. für Wasserbau u. Wassermengenwirtschaft im Inst. für Bauingenieurwesen IV 1987. Institut für Wasserbau und Wassermengenwirtschaft und Versuchsanstalt für Wasserbau Oskar v. Miller-Institut in Obernach, Bericht Nr. 57, Technische Universität München, Munich, Obernach, Germany.
Knoll, F.G., 1999. Radiation Detection and Measurements, third ed. J. Wiley & Sons, Inc.
Liritzis, I., (PhD thesis) 1979. Thermoluminescence and $^{230}Th/^{234}U$ Dating Investigations of Hellenic Materials. University of Edinburgh, Dept. of Physics, Scotland (269 p.).
Liritzis, I., 2010. Strofilas (Andros Island, Greece): New evidence of Cycladic Final Neolithic dated by novel luminescence and Obsidian Hydration methods. J. Archaeol. Sci. 37, 1367–1377.
Liritzis, I., 2011. Surface dating by luminescence: an overview. Geochronometria 38 (3), 292–302.

Liritzis, I., Zacharias, N., 2011. Portable XRF of archaeological artefacts: current research, potential and limitations. In: Shackley, S. (Ed.), X ray Fluorescence Spectrometry in Geoarchaeology. Natural Sciences in Archaeological Series. Springer, North America, pp. 109–142.
Liritzis, I., Vafiadou, A., 2012. Calibration aspects of thick source alpha counter ZnS system. Measurements 45 (8), 1966–1980.
Liritzis, I., Foti, F., Guibert, P., Schvoerer, M., 1996. Solar bleaching of thermoluminescence of calcites. Nucl. Instr. Meth. B 117, 260–268.
Liritzis, I., Bakopoulos, Y., 1997. Functional behaviour of solar bleached thermoluminescence in calcites. Nucl. Instr. Meth. B 132, 87–92.
Liritzis, I., Guilbert, P., Foti, F., Schvoerer, M., 1997. The Temple of Apollo (Delphi) strengthens new thermoluminescence dating method. Geoarchaeol. Int. 12 (5), 479–496.
Liritzis, I., Katsanopoulou, D., Soter, S., Galloway, R.B., 2001. In search of ancient Helike Gulf of Corinth, Greece. J. Coastal Res. 17 (1), 118–123.
Liritzis, I., Kitis, G., Galloway, R.B., Vafiadou, A., Tsirliganis, N., Polymeris, G., 2008. Probing luminescence dating of archaeologically significant carved rock types. Mediterr. Archaeol. Archaeom. 8 (1), 61–79.
Liritzis, I., Drivaliari, A., Polymeris, G., Katagas, C., 2010. New quartz technique for OSL dating of limestones. Mediterr. Archaeol. Archaeom. 10 (1), 81–87.
Liritzis, I., Singhvi, A.K., Feathers, J.K., Wagner, G.A., Kadereit, A., Zacharias, N., Li, S.-H., 2013a. Luminescence Dating in Archaeology, Anthropology and Geoarchaeology: an Overview. Springer Briefs in Earth System Sciences. Springer, Heidelberg http://link.springer.com/content/pdf/10.1007/978-3-319-00170-8.pdf
Liritzis, I., Stamoulis, K., Papachristodoulou, C., Ioannides, K., 2013b. A re-evaluation of radiation dose rate conversion factors. Mediterr. Archaeol. Archaeom. 13 (3), 1–15.
Maniatis, Y., Tite, M., 1981. Technological examination of Neolithic-Bronze Age pottery from central and southeast Europe and from the Near East. J. Archaeol. Sci. 8, 59–76.
Michaud, J.P., 1972. Koumoula. BCH 96, 912–913.
Murray, A.S., Wintle, A.G., 2000. Luminescence dating of quartz using an improved single – aliquot regenerative – dose protocol. Radiat. Meas. 32, 57–73.
Müller, S., 1992. Delphes et sa région à l'époque mycénienne. BCH 116, 445–495.
Picon, M., 1976. Remarques preliminaries sur deux types d'altération de la composition chimique des céramiques au cours du temps. Figlina 1, 159–166.
Pagonis, V., Chen, R., Kitis, G., 2011. On the intrinsic accuracy and precision of luminescence dating techniques for fired ceramics. J. Archaeol. Sci. 38, 1591–1602.
Polymeris, G.S., Kitis, G., Liolios, A.K., Sakalis, A., Zioutas, K., Anassontzis, E.G., Tsirliganis, N.C., 2009. Luminescence dating of the top of a deep water core from the NESTOR site near the Hellenic Trench, East Mediterranean Sea. Quat. Geochronol. 4, 68–81.
Polymeris, G.S., Afouxenidis, D., Raptis, S., Liritzis, I., Tsirliganis, N.C., Kitis, G., 2011. Relative response of TL and component-resolved OSL to alpha and beta radiations in annealed sedimentary quartz. Radiat. Meas. 46, 1055–1064.
Prescott, J.R., Hutton, J.T., 1988. Cosmic ray and gamma ray dosimetry for TL and ESR. Nuclear Tracks and Radiation Measurements 14., pp. 223–227.
Roberts, H.M., Wintle, A.G., 2001. Equivalent dose determinations for polymineralic fine grains using the SAR protocol: application to a Holocene sequence of the Chinese Loess Plateau. Quat. Sci. Rev. 20, 859–863.
Singhvi, A.K., Sharma, Y.P., Agrawal, D.P., 1982. Thermoluminescence dating of sand dunes in Rajasthan, India. Nature 295, 313–315.
Solongo, S., Richter, D., Begzjav, T., Hublin, J.-J., 2014. OSL and TL characteristics of fine grain quartz from Mongolian prehistoric pottery used for dating. Geochronometria 41 (1), 15–23.
Stokes, S., Ingram, S., Aitken, M.J., Sirocko, F., Anderson, R., Leuschner, D., 2003. Alternative chronologies for Late Quaternary (Last Inerglacial – Holocene) deep sea sediment via optical dating of silt – size quartz. Quat. Sci. Rev. 22, 925–941.
Theocaris, P., Liritzis, I., Lagios, E., Sampson, A., 1997. Geophysical prospection and archaeological test excavation and dating in two Hellenic pyramids. Surv. Geophys. 17, 593–618.
Theocaris, P.S., Liritzis, I., Galloway, R.B., 1994. Dating of two Hellenic pyramids by a novel application of thermoluminescence. J. Archaeol. Sci. 24, 399–405.
Thomas, P.J., Nagabhushanam, P., Reddy, D.V., 2008. Optically stimulated luminescence dating of heated materials using single-aliquot regenerative dose procedure: a feasibility study using archaeological artefacts from India. J. Archaeol. Sci. 35 (3), 781–790.
Touchais, G., 1981. L'Antre corycien I. BCH Suppl. VII, 183–193 (170172) http://www.persee.fr/web/revues/home/prescript/issue/bch_0304-2456_1981_sup_7_1
Vafiadou, A., Murray, M.S., Liritzis, I., 2007. Optically stimulated luminescence (OSL) dating investigations of rock and underlying soil from three case studies. J. Archaeol. Sci. 34 (10), 1659–1669.
Wagner, G.A., 1998. Age Determination of Young Rocks and Artifacts: Physical and Chemical Clocks in Quaternary Geology and Archaeology. Springer–Verlag, Berlin Heidelberg.
Wallinga, J., 2002. Optically stimulated luminescence dating of fluvial deposits: a review. Boreas 31, 303–322.
Zacharias, N., Buxeda i Garrigos, J., Mommsen, H., Schwedt, A., Kilikoglou, V., 2005. Implications of burial alterations on luminescence dating of archaeological ceramics. J. Archaeol. Sci. 32.1, 49–57.
Zacharias, N., Michael, C.T., Philaniotou-Hadjiannastasiou, O., Hein, A., Bassiakos, Y., 2006a. Fine grain TL dating of archaeometallurgical furmace walls. J. Cult. Herit. 7, 23–29.
Zacharias, N., Michael, C.T., Georgakopoulou, M., Kilikoglou, V., Bassiakos, Y., 2006b. Quartz TL dating on selected layers from archaeometallurgical kiln fragments: a proposed procedure to overcome age dispersion. Geochronometria 25, 29–36.
Zhang, J.F., Zhou, L.P., 2007. Optimization of the 'double SAR' procedure for polymineral fine grains. Radiat. Meas. 42, 1475–1482.
Zimmerman, D.W., 1971. Luminescence dating using fine grains from pottery. Archaeometry 13 (1), 29–56.